



The effect of indirect UV/ozone treatment on pentacene thin film transistors with double-stacked organic gate insulators

Min Su Kim^a, Dong-Hoon Lee^a, Hyeong Jun Cho^a, Jongsu Oh^a, So Young Lee^a, Jae Moon Kim^a, KeeChan Park^b, Yong-Sang Kim^{a,*}

^a School of Electronic and Electrical Engineering, Sungkyunkwan University, Suwon, Gyeonggi, 16419, South Korea

^b Department of Electronics Engineering, Konkuk University, Seoul, 05029, South Korea

ARTICLE INFO

Keywords:

Organic thin film transistor
Pentacene
Indirect UV/ozone treatment

ABSTRACT

We investigated the indirect UV/ozone treatment, which means treating the insulator surface under tens of nanometers, rather than the direct surface of the insulator. The double-stacked organic layers are used as gate insulator and the UV/ozone treatment is conducted between these two layers. We analyzed the surface morphologies of the gate insulator and the pentacene by atomic force microscopy (AFM) to confirm the effect of indirect UV/ozone treatment. The UV/ozone treatment reduced the surface roughness of the upper side gate insulator and increased the pentacene grain size. Pentacene-based thin film transistors were fabricated and the electrical property improvement after this treatment was examined. The largest improvement was found when the UV/ozone treatment time is 10 min and the upper side gate insulator thickness is 20 nm, and the mobility at that condition is 1.21 cm²/V s, which is larger than three times that without UV/ozone treatment (0.33 cm²/V s).

1. Introduction

Organic thin film transistors (TFTs) have received a lot of attention for the potential application to flexible electronics, such as sensor, memory, light-emitting diode, and switching device for active-matrix flat-panel displays (AMFPD) [1–5] because organic TFTs can be fabricated on the plastic substrate owing to their low processing temperature and ability to endure mechanical bending stress [6–9].

Pentacene (C₂₂H₁₄) is the most commonly used active material in organic TFTs. The electrical characteristics of pentacene-based organic TFTs, such as field-effect mobility, are comparable to amorphous silicon thin film transistors (a-Si TFTs), which are commonly used for backplane of liquid crystal displays (LCD) but they are quite inferior compared to general inorganic TFTs. So, it is necessary to improve electrical characteristics for high-performance flexible electronics.

The electrical characteristics of organic TFTs are closely related to the interface characteristics between gate insulator layer and active layer. Therefore, there were many efforts to improve the interface characteristics with various direct treatment on the surface of gate dielectric layer, such as O₂-plasma treatment, hexamethyldisilane (HMDS) treatment, octadecyltrichlorosilane (OTS) treatment, etc [10–12].

The UV/ozone treatment was also used as surface treatment method on gate insulator layer. When a polymer gate dielectric layer is treated

with UV/ozone, the surface energy increases because some of the surface polymer chains are broken and they are combined with oxygen atoms forming polar groups, such as –OH, –CO–, –COOH, etc [13,14]. The increased surface energy after UV/ozone treatment makes pentacene grow vertically, resulting in large pentacene grains [15,16]. Organic TFT with large pentacene grains has higher mobility compared to that with small pentacene grains, because the former has fewer grain boundaries and so fewer boundary scattering than the latter. A large increase in mobility (0.07 cm²/V s to 2.66 cm²/V s) after direct UV/ozone treatment on polymer gate insulator was reported in Ref. [15]. However, the hysteresis was also increased from 0.5 V to 24.9 V after treatment because the hydroxyl (OH) groups generated by the UV/ozone treatment act as electron trap sites at the organic semiconductor/gate dielectric interface. Here we also analyzed the effect of the direct UV/ozone treatment on poly(4-vinylphenol-co-methyl methacrylate) (PVP-co-PMMA) gate dielectric. Fig. S1(a)–(b) show the transfer characteristics measured in two opposite gate voltage sweep directions: (a) without UV/ozone treatment and (b) with direct UV/ozone treatment. We defined the hysteresis as the difference of gate-to-source voltage (V_{GS}) when the drain-to-source current (I_{DS}) is –10⁷ A. In our case, the mobility was increased from 0.25 cm²/V s to 1.21 cm²/V s and the hysteresis was increased from 0.18 V to 17.73 V after 10 min of the direct UV/ozone treatment.

Not only the surface energy, but the roughness of gate insulator

* Corresponding author.

E-mail address: yongsang@skku.edu (Y.-S. Kim).

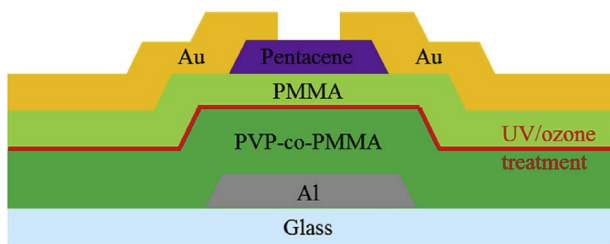


Fig. 1. The pentacene-based organic TFT structure using PMMA/PVP-co-PMMA as gate insulators.

surface is also an important factor that determines the size of pentacene grains. The mobilities of pentacene TFTs with smooth gate insulator surface is larger than those with rough gate insulator surface because the pentacene grains grow bigger on the smooth surface [13,17–19].

In this study, we propose the indirect UV/ozone treatment method that UV/ozone treatment is executed below the gate insulator surface. We improved the electrical performance of pentacene-based organic TFTs without increasing the hysteresis by this method of reducing the gate insulator surface roughness and enlarging the pentacene grains which are deposited on the surface.

2. Experiments

The structure of organic TFT is shown in Fig. 1. The glass substrate was cleaned with acetone, isopropyl alcohol and deionized water in an ultrasonic cleaner. Al gate electrode was deposited on the substrate through a shadow mask by thermal evaporation to a thickness of 100 nm. We used two kinds of solution processed organic gate insulators. Poly(4-vinylphenol-co-methyl methacrylate) (PVP-co-PMMA), the bottom insulator layer, was spin-coated to a thickness of 130 nm. Prior to spin-coating poly(methyl methacrylate) (PMMA), the top insulator layer, we did UV/ozone treatment (with a wave length of 253.7 nm) for various times: 0, 2.5, 5 and 10 min. The water contact angle measurements were carried out on the UV/ozone treated PVP-co-PMMA surfaces to investigate the changes of surface properties. PMMA was spin-coated on the UV/ozone treated substrate, to various thicknesses: 20, 60, 160 and 200 nm. The PMMA thickness was controlled by adjusting solution concentration. The 70 nm pentacene active layer was deposited on the PMMA through a shadow mask at a deposition rate of 0.2–0.3 Å/s with a substrate temperature of 80 °C. The 100 nm Au source/drain electrodes were deposited by thermal evaporation through a shadow mask. The width (W) and length (L) of the pentacene TFTs in this experiment are 1000 μm and 100 μm, respectively.

The surface morphologies of PMMA and pentacene were characterized by using atomic force microscopy (AFM) system (PSIA XE-100) in non-contact mode and the electrical characteristics of pentacene TFTs were measured by using semiconductor parameter analyzer (HP4145B).

3. Results and discussion

3.1. UV/ozone treatment effect with different treatment time

To optimize the UV/ozone treatment time, we measured the water contact angles on the UV/ozone treated PVP-co-PMMA surfaces with various treatment times. Fig. 2 shows the relation between UV/ozone treatment time and the water contact angle on the PVP-co-PMMA layer. As treatment time increased from 0 min to 5 min, the water contact angle was decreased from 88.3° to 29.6°. We can infer that the change in the water contact angle leads to a change in the surface energy from the following equation [14,20].

$$(1 + \cos \theta)\gamma_L = 2(\gamma_S^d \gamma_L^d)^{1/2} + 2(\gamma_S^p \gamma_L^p)^{1/2} \quad (1)$$

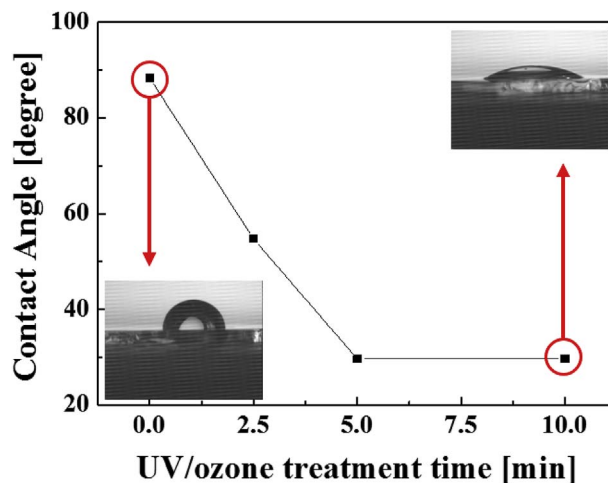


Fig. 2. The relationship between the UV/ozone treatment time and the water contact angle. The insets are the water contact angle images on the initial and UV/ozone treated PVP-co-PMMA.

γ_L is the surface energy of the liquid used for measurement and it is the sum of γ_L^d and γ_L^p , which represent the dispersed part and the polar part, respectively. The total surface energy γ_S can be estimated as the following equation.

$$\gamma_S \cong \gamma_S^d + \gamma_S^p \quad (2)$$

In equation (2), γ_S^d is the dispersed component and γ_S^p is the polar component of the solid surface energy. The decreased water contact angle means the increase of γ_S^p , so the increase of the total surface energy γ_S [14]. There was no further decrease in the water contact angle after 5 min, but we optimized the UV/ozone treatment time to 10 min for sufficient treatment.

We spin-coated PMMA with a thickness of 20 nm on the UV/ozone treated or untreated PVP-co-PMMA layer. The relationship between the root-mean-square (RMS) roughness of PMMA and the UV/ozone treatment time is shown in Fig. 3. The surface roughness of PMMA decreases from 0.312 nm to 0.193 nm as UV/ozone treatment time increases from 0 min to 10 min. In many studies, the UV/ozone treatment has been used to remove substrate contaminants and to increase coating uniformity thereon. C.N. Li et al. [20] reported that the surface roughness of the deposited NPB is smoother on the UV/ozone treated ITO (RMS = 0.72 nm) than on the untreated one (RMS = 2.71 nm). The UV/ozone treatment on the PVP-co-PMMA also has an effect on reducing the

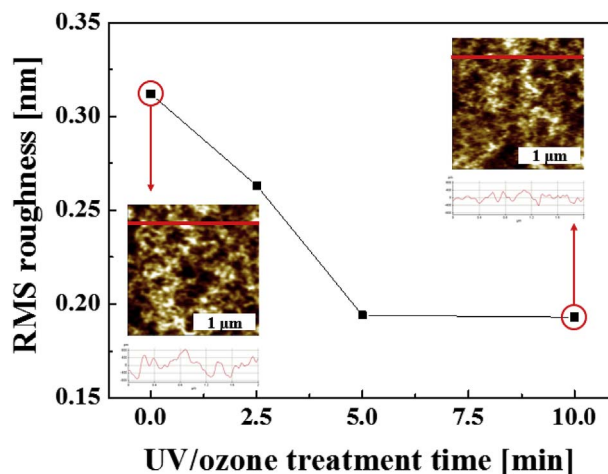


Fig. 3. The relationship between the UV/ozone treatment time and the PMMA RMS roughness when PMMA thickness is 20 nm. The insets are AFM images of PMMA surface and line profiles.

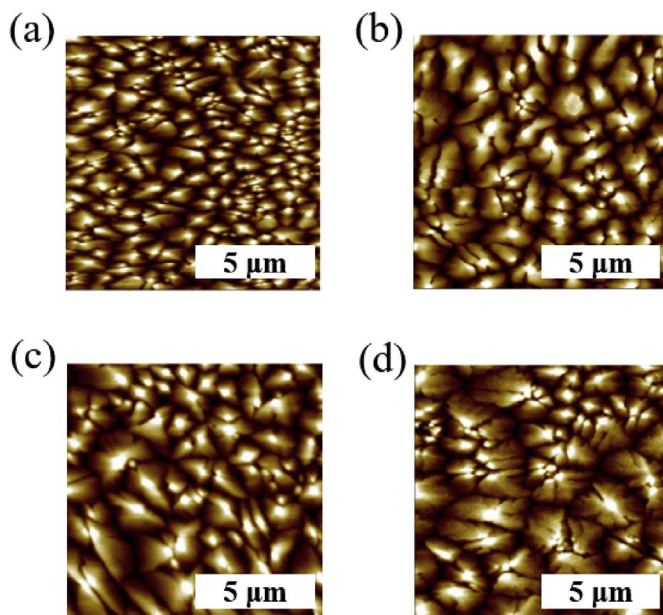


Fig. 4. The AFM images of pentacene morphology when PMMA thickness is 20 nm. The UV/ozone treatment times are (a) 0 min, (b) 2.5 min, (c) 5 min and (d) 10 min.

PMMA surface roughness on it. It can be explained that the PMMA chains are aligned in the same direction by the surface dipoles generated by the UV/ozone treatment. The insets in Fig. 3 are AFM images measured in $2 \mu\text{m} \times 2 \mu\text{m}$ size and the corresponding line profiles. We can also see through the AFM images and the line profiles that the PMMA surface roughness has been decreased after UV/ozone treatment.

Fig. 4 shows the AFM images of pentacene grains when they are deposited on PMMA with various UV/ozone treatment times. The pentacene grain size increases when the UV/ozone treatment time increases at a PMMA thickness of 20 nm, as shown in Fig. 4(a)–(d). It is strongly related to the previous results of PMMA roughness we mentioned in Fig. 3. The pentacene can grow well on the smooth and ordered surface [13,17–19], so the pentacene grain size is greatest when the PMMA RMS roughness is the minimum (0.193 nm) at 10 min of UV/ozone treatment. The UV/ozone treatment below PMMA reduces the surface roughness of PMMA and it indirectly affects the size of pentacene grains because the pentacene grain size is affected by the roughness of the surface on which it is deposited. As the UV/ozone treatment time increases, the surface of PMMA gets ordered and smoother so the pentacene can grow well with large grain size.

We investigated the effect of indirect UV/ozone treatment to pentacene TFTs and the transfer curves with various UV/ozone treatment times are shown in Fig. 5(a). The sweep range of gate-to-source voltage (V_{GS}) is from +20 V to -40 V and the drain-to-source voltage (V_{DS}) is -20 V. As shown in Fig. 5(a), the on-current increases as the UV/ozone treatment time increases. The drain-to-source current (I_{DS}) in the saturation mode can be represented as

$$I_{DS} = \frac{W}{2L} C_i \mu (V_{GS} - V_T)^2 \quad (3)$$

where W is the channel width, L is the channel length, C_i is the capacitance of the gate insulator, μ is the mobility and V_T is the threshold voltage. We calculated the mobilities by equation (3) and the relationship between the mobility and the UV/ozone treatment time is shown in Fig. 5(b). The mean values of the mobility were extracted from four samples per each condition. The mobility without UV/ozone treatment is $0.33 \text{ cm}^2/\text{V s}$. The mobility increases as UV/ozone treatment time increases from 0 to 5 min and it is almost saturated after 5 min. The huge increase in mobility is due to the smooth PMMA

roughness and the large pentacene grains. Both the smooth roughness of gate insulator surface and the large pentacene grains decrease scattering when charge carriers pass through the channel [15–19]. The final mobility is $1.21 \text{ cm}^2/\text{V s}$ when the UV/ozone treatment time is 10 min. Other electrical characteristics such as the threshold voltage and the on/off current ratio as well as the mobility are shown in Table 1. The relationship between the threshold voltage and the UV/ozone treatment is shown in Fig. S2. The threshold voltage was shifted in the positive direction as the organic contamination was removed after UV/ozone treatment. However, since the threshold voltage is influenced by various factors such as the experimental environment, further elaborative experiment and analysis are needed to understand the exact mechanism.

3.2. UV/ozone treatment effect with different PMMA thickness

The relationship between PMMA roughness and the PMMA thickness, when the UV/ozone treatment time is 10 min, is shown in Fig. 6. The surface roughness of PMMA increases when the PMMA thickness increases. It means that the effect of the UV/ozone treatment decreases when it goes far from the UV/ozone treated surface. The PMMA RMS roughness when PMMA thickness is 200 nm (0.312 nm) is same with that without treatment in Fig. 3 (0.312 nm). This means that the treatment effect no longer appears when the thickness of the PMMA is more than 200 nm. The insets are AFM images measured in $2 \mu\text{m} \times 2 \mu\text{m}$ size and the corresponding line profiles when the PMMA thicknesses are 20 nm and 200 nm respectively.

The pentacene grain size decreases with same UV/ozone treatment time (10 min) when the PMMA thickness increases, as shown in Fig. 7(a)–(d). The results for pentacene grains are inversely related to the previous PMMA roughness results shown in Fig. 6. It is because the pentacene grains grow smaller on the rough surface.

The transfer curves without UV/ozone treatment (black line) and with 10 min of UV/ozone treatment (red line) with various PMMA thicknesses are shown in Fig. 8(a) and (b). The PMMA thicknesses are (a) 20 nm and (b) 200 nm. The sweep range of gate-to-source voltage (V_{GS}) is from +20 V to -40 V and the drain-to-source voltage (V_{DS}) is -20 V. The increase in on-current is largest when the PMMA is 20 nm and decreases with increasing PMMA thickness.

From the transfer curves in Fig. 8(a) and (b), however, we cannot directly compare the mobility changes by the PMMA thickness variation because the I_{DS} is proportional to both the mobility and the capacitance of the gate insulator. The reduction in on-current is affected not only by the mobility reduction but also by the reduction of the capacitance due to the increase in PMMA thickness. So, we also calculated the mobilities by equation (3) to see only the effect of PMMA thickness on mobility. Fig. 8(c) shows the relation between the mobility and the PMMA thickness without UV/ozone treatment and with 10 min of treatment. The mean values of the mobility were extracted from four samples per each condition. When the treatment is not applied, mobility is almost same ($0.33 \pm 0.02 \text{ cm}^2/\text{V s}$) even though the PMMA thickness is increased. It is because the PMMA surface roughness and the pentacene grain size are almost same for the untreated samples, as shown in Fig. S4. However, the mobility increases after 10 min of treatment and the increment decreases when the PMMA thickness increase because the effect of UV/ozone treatment decreases as the surface moves away from the treated point. The relationship between the threshold voltage and the PMMA thickness is shown in Fig. S3. The threshold voltage shifted in the negative direction as the PMMA thickness increased.

All the results are summarized in Table 1. From the AFM results of the PMMA surface roughness and the pentacene morphology and electrical characteristics of the pentacene TFTs, we can verify the effect of indirect UV/ozone treatment to pentacene TFTs. The UV/ozone treatment tens of nanometers below the surface of the gate insulator indirectly affects the size of pentacene grains by modifying the surface

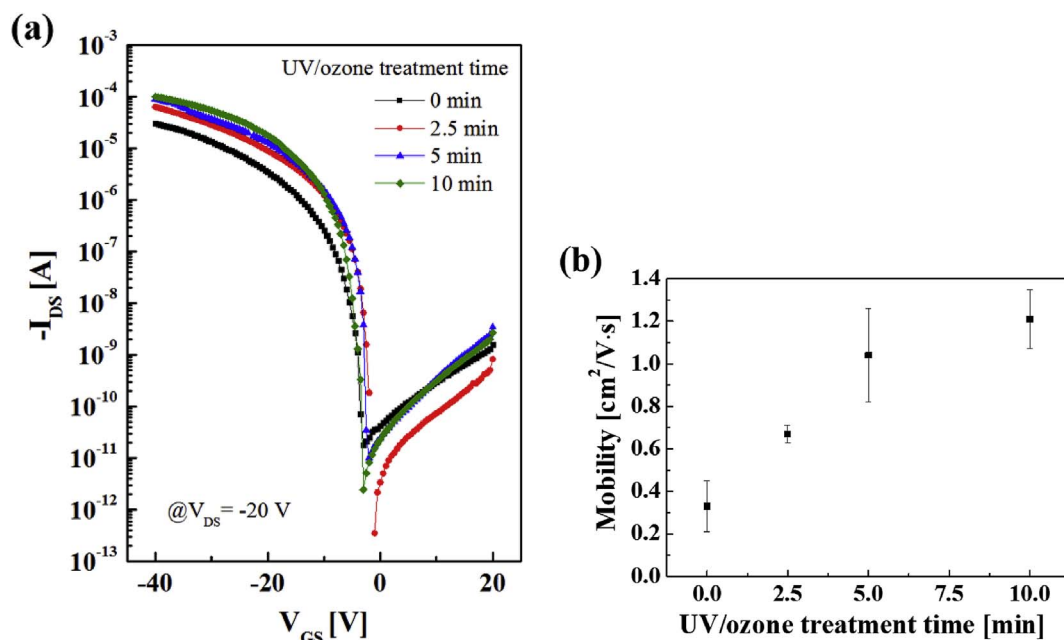


Fig. 5. (a) I_{DS} - V_{GS} characteristics with various UV/ozone treatment times (0, 2.5, 5 and 10 min) and (b) relationship between the mobility and the UV/ozone treatment time when the PMMA thickness is 20 nm.

Table 1

The contact angle on the PVP-co-PMMA, the PMMA RMS roughness, the pentacene grain size and the mean electrical parameters extracted from four each sample with UV/ozone treatment time and PMMA thickness.

UV/ozone treatment time [min]	PMMA thickness [nm]	Contact angle on PVP-co-PMMA [°]	PMMA RMS roughness [nm]	Pentacene grain size [μm]	Mobility [cm ² /V s]	Threshold voltage [V]	On/off ratio [A/A]
0	20	88.3	0.312	< 1	0.33	-10.80	6.7×10^5
2.5	20	54.7	0.263	1-2	0.67	-6.75	1.0×10^8
5	20	29.6	0.194	2-3	1.04	-7.92	4.7×10^7
10	20	29.6	0.193	> 3	1.21	-7.50	1.5×10^7
10	60	29.6	0.236	2-3	0.77	-7.83	1.0×10^8
10	160	29.6	0.280	< 1	0.48	-10.92	1.6×10^8
10	200	29.6	0.312	< 1	0.39	-11.63	6.9×10^7

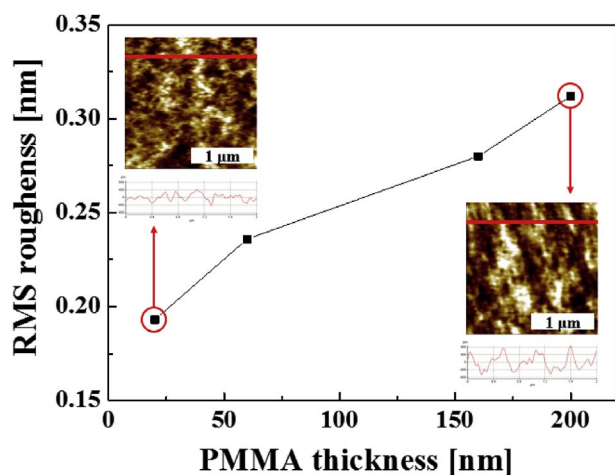


Fig. 6. The relationship between the PMMA thickness and the PMMA RMS roughness when UV/ozone treatment time is 10 min. The insets are AFM images of PMMA surface and line profiles.

roughness of the gate insulator. Both the large pentacene grain size and the smooth gate insulator roughness by this indirect UV/ozone treatment method increase the mobility of pentacene TFT. The mobility increases when the treatment time increases and the upper insulator thickness decreases. When the treatment time was 10 min and the

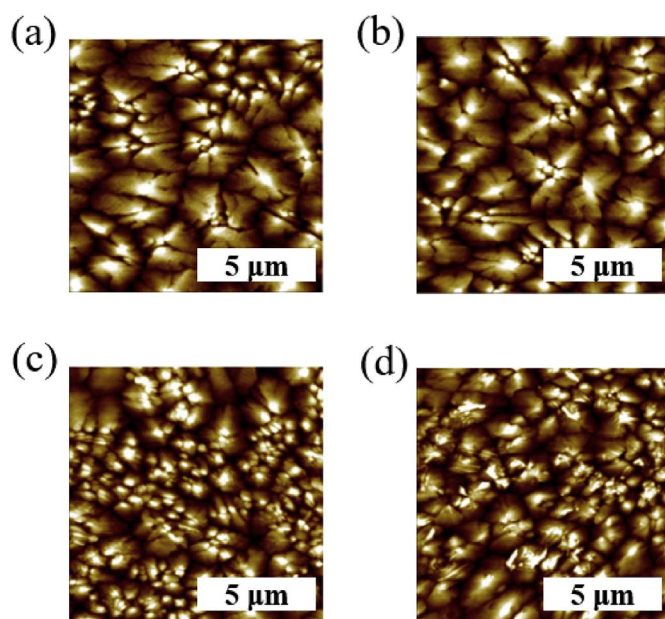


Fig. 7. AFM images of pentacene grains when UV exposure time is 10 min. PMMA thicknesses are (a) 20 nm, (b) 60 nm, (c) 160 nm and (d) 200 nm.

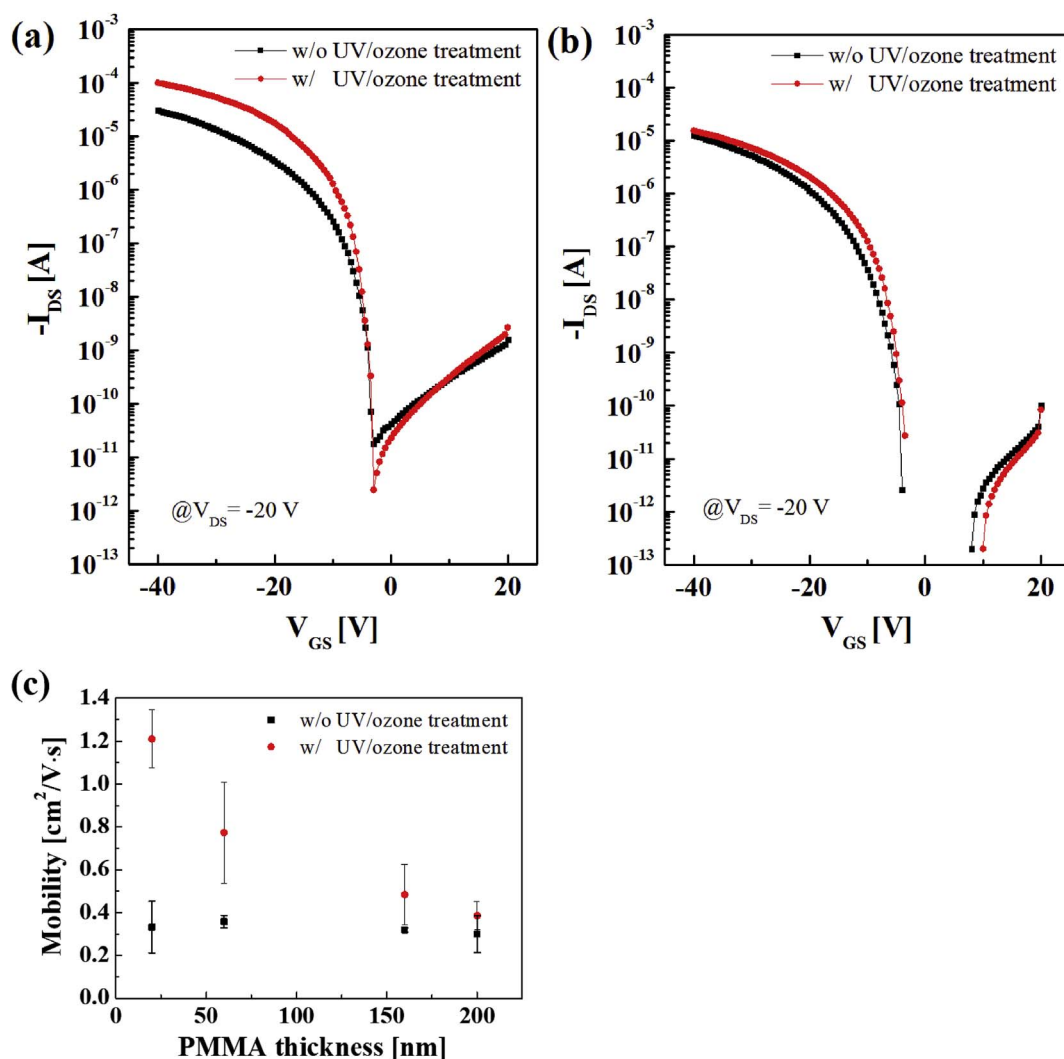


Fig. 8. I_{DS} - V_{GS} characteristics with 10 min of UV/ozone treatment (red line) and without UV/ozone treatment (black line) when the PMMA thicknesses are (a) 20 nm and (b) 200 nm. (c) The relationship between the mobility and the PMMA thickness without (black line) and with (red line) 10 min of UV/ozone treatment. (For interpretation of the references to colour in this figure legend, the reader is referred to the web version of this article.)

PMMA thickness was 20 nm, the mobility was the largest ($1.21 \text{ cm}^2/\text{V s}$) without any severe hysteresis increase (3.28 V), as shown in Fig. S1(c).

4. Conclusion

We used the indirect UV/ozone treatment method to improve the electrical performance of pentacene TFTs. The effectiveness of this method is verified with pentacene TFTs using PMMA/PVP-co-PMMA as double stacked gate insulator materials. We investigated the water contact angle, the PMMA surface roughness, the pentacene grain size, and the electrical characteristics varying the UV/ozone treatment times and the PMMA thicknesses. When the treatment time increases, the PMMA surface roughness decreases and the pentacene grain size increases, so the mobility increases. However, the effect of UV/ozone treatment decreases when the PMMA thickness increases. The largest mobility of the pentacene TFT was found when the treatment time is 10 min and the PMMA thickness is 20 nm. The final mobility is $1.21 \text{ cm}^2/\text{V s}$ which is more than three times higher than without UV/ozone treatment ($0.33 \text{ cm}^2/\text{V s}$).

Appendix A. Supplementary data

Supplementary data related to this article can be found at <http://dx.doi.org/10.1016/j.orgel.2017.10.036>.

References

- [1] X. Yu, N. Zhou, S. Han, H. Lin, D.B. Buchholz, J. Yu, R.P.H. Chang, T.J. Marks, A. Facchetti, Flexible spray-coated TIPS-pentacene organic thin-film transistors as ammonia gas sensors, *J. Mater. Chem. C* 1 (2013) 6532.
- [2] P. Cosseddu, S. Lai, G. Casula, L. Raffo, A. Bonfiglio, High performance, foldable, organic memories based on ultra-low voltage, thin film transistors, *Org. Electron.* 15 (2014) 3595–3600.
- [3] F. Adriyanto, C.-K. Yang, T.-Y. Yang, C.-Y. Wei, Y.-H. Wang, Solution-processed barium zirconate titanate for pentacene-based thin-film transistor and memory, *IEEE Electron Device Lett.* 34 (2013) 1241–1243.
- [4] Q. Zhang, B. Li, S. Huang, H. Nomura, H. Tanaka, C. Adachi, Efficient blue organic light-emitting diodes employing thermally activated delayed fluorescence, *Nat. Photonics* 8 (2014) 326–332.
- [5] E. Song, H. Nam, Low power programmable shift register with depletion mode oxide TFTs for high resolution and high frame rate AMFPDs, *J. Disp. Technol.* 10 (2014) 834–838.
- [6] C.-L. Fan, W.-C. Lin, H.-H. Peng, Y.-Z. Lin, B.-R. Huang, Correlation between ambient air and continuous bending stress for the electrical reliability of flexible pentacene-based thin-film transistors, *Jpn. J. Appl. Phys.* 54 (2015) 011602.
- [7] C.B. Park, K.M. Kim, J.E. Lee, H. Na, S.S. Yoo, M.S. Yang, Flexible electrophoretic display driven by solution-processed organic TFT with highly stable bending feature, *Org. Electron.* 15 (2014) 3538–3545.

- [8] J. Lee, D.K. Hwang, J.-M. Choi, K. Lee, J.H. Kim, S. Im, J.H. Park, E. Kim, Flexible semitransparent pentacene thin-film transistors with polymer dielectric layers and NiOx electrodes, *Appl. Phys. Lett.* 87 (2005) 023504.
- [9] Q. Cao, Z.-T. Zhu, M.G. Lemaitre, M.-G. Xia, M. Shim, J.A. Rogers, Transparent flexible organic thin-film transistors that use printed single-walled carbon nanotube electrodes, *Appl. Phys. Lett.* 88 (2006) 113511.
- [10] S.C. Lim, S.H. Kim, J.H. Lee, M.K. Kim, D.J. Kim, T. Zyung, Surface-treatment effects on organic thin-film transistors, *Synth. Met.* 148 (2005) 75–79.
- [11] A. Virkar, S. Mannsfeld, J.H. Oh, M.F. Toney, Y.H. Tan, G.-y. Liu, J.C. Scott, R. Miller, Z. Bao, The role of OTS density on pentacene and C60 nucleation, thin film growth, and transistor performance, *Adv. Funct. Mater.* 19 (2009) 1962–1970.
- [12] S. Wang, J.-H. Kim, E.-K. Park, J. Oh, K. Park, Y.-S. Kim, Two-step surface modification for bottom-contact structured pentacene thin-film transistors, *Org. Electron.* 43 (2017) 21–26.
- [13] K. Shin, S.Y. Yang, C. Yang, H. Jeon, C.E. Park, Effects of polar functional groups and roughness topography of polymer gate dielectric layers on pentacene field-effect transistors, *Org. Electron.* 8 (2007) 336–342.
- [14] H.-W. Zan, C.-W. Chou, Effect of surface energy on pentacene thin-film growth and organic thin film transistor characteristics, *Jpn. J. Appl. Phys.* 48 (2009) 031501.
- [15] J.B. Koo, S.Y. Kang, I.K. You, K.S. Suh, Effect of UV/ozone treatment on hysteresis of pentacene thin-film transistor with polymer gate dielectric, *Solid-State Electron.* 53 (2009) 621–625.
- [16] S.J. Han, J.-H. Kim, J. Won Kim, C.-K. Min, S.-H. Hong, D.-H. Kim, K.-H. Baek, G.-H. Kim, L.-M. Do, Y. Park, Effects of UV/ozone treatment of a polymer dielectric surface on the properties of pentacene thin films for organic transistors, *J. Appl. Phys.* 104 (2008) 013715.
- [17] S. Steudel, S.D. Vusser, S.D. Jonge, D. Janssen, S. Verlaak, J. Genoe, P. Heremans, Influence of the dielectric roughness on the performance of pentacene transistors, *Appl. Phys. Lett.* 85 (2004) 4400.
- [18] S.E. Fritz, T.W. Kelley, C.D. Frisbie, Effect of dielectric roughness on performance of pentacene TFTs and restoration of performance with a polymeric smoothing layer, *J. Phys. Chem.* 109 (2005) 10574–10577.
- [19] Y. Kato, S. Iba, R. Teramoto, T. Sekitani, T. Someya, H. Kawaguchi, T. Sakurai, High mobility of pentacene field-effect transistors with polyimide gate dielectric layers, *Appl. Phys. Lett.* 84 (2004) 3789–3791.
- [20] C.N. Li, C.Y. Kwong, A.B. Djurisic, P.T. Lai, P.C. Chui, W.K. Chan, S.Y. Liu, Improved performance of OLEDs with ITO surface treatments, *Thin Solid Films* 477 (2005) 57–62.